ELSEVIER

International Journal of Mass Spectrometry 184 (1999) 145–152

International Journal of Mass Spectrometry

The half-life of ^{126}Sn refined by thermal ionization mass spectrometry measurements

Felix Oberli[a,*], Philipp Gartenmann[b], Martin Meier[a], Walter Kutschera[c], Martin Suter[b], Gerhard Winkler[c]

[a]*Institut für Isotopengeologie und Mineralische Rohstoffe, ETH Zentrum, CH-8092 Zürich, Switzerland*
[b]*Institut für Teilchenphysik, ETH Hönggerberg, CH-8093 Zürich, Switzerland*
[c]*Institut für Radiumforschung und Kernphysik der Universität Wien, A-1090 Wien, Austria*

Received 7 April 1998; accepted 1 December 1998

Abstract

Recently, Haas et al. [Nucl. Instrum. Methods Phys. Res. B 114 (1996) 131] have determined the half-life of ^{126}Sn by combining measurements of activity concentration (by gamma counting) and isotope abundance [by accelerator mass spectrometry (AMS)]. A new determination of the isotope abundance of ^{126}Sn in the same material by thermal ionization mass spectrometry (TIMS) is reported, which minimizes the error contribution to the overall uncertainty of the decay constant. The greatly improved value for the half-life of ^{126}Sn $(2.345 \pm 0.071) \times 10^5$ a (1σ), is consistent with the less precise determination partly based on AMS, and with an independent measurement by Zhang et al. [J. Radioanal. Nucl. Chem. 212 (1996) 93] partly based on a fission yield estimate. A value of $(5.2849 \pm 0.0017) \times 10^{-5}$ (95% confidence level) is reported for ^{234}U/^{238}U in the National Bureau of Standards Standard Reference Material (SRM) 960/New Brunswick Laboratory Certified Reference Material (CRM) 112a uranium standard. (Int J Mass Spectrom 184 (1999) 145–152) © 1999 Elsevier Science B.V.

Keywords: ^{126}Sn; Decay constant; Half-life; Mass spectrometry; TIMS

1. Introduction

The abundance of long-lived radionuclides and their daughter products provides information on the chemical evolution of the system where they are found. Knowledge of the decay constants for these radionuclides permits to quantify evolutionary histories at time scales, which are comparable to their half-lives.

Because the half-life of ^{126}Sn is short as compared to the age of the solar system, there is no ^{126}Sn left from nucleosynthesis. ^{126}Sn in the present terrestrial environment is therefore limited to contributions from spontaneous fission of ^{238}U and to anthropogenic input. For a secular equilibrium ratio of ^{126}Sn/Sn = $\sim 10^{-14} \times$ U/Sn [1] and average concentrations for U and Sn of 2.8 and 5.5 ppm, respectively [2], ^{126}Sn/Sn in the upper continental crust is $\sim 10^{-14}$–10^{-15}, well below the detection limit of modern radiochemical methods. On the other hand, because of its relatively long half-life, ^{126}Sn derived from nuclear weapons testing, released by spent fuel reprocessing plants or potentially leaked from nuclear waste dis-

* Corresponding author. E-mail: oberli@erdw.ethz.ch

PII S1387-3806(98)14281-1

posal sites, is considered a hazard to the environment [3]. In contrast to other well known fission nuclides, such as ^{90}Sr or ^{137}Cs, which are characterized by much shorter half-lives and two orders of magnitude higher production rates, ^{126}Sn is exceedingly difficult to monitor. Its presence in contaminated areas had to be inferred from the detection of its proxy, ^{121m}Sn ($T_{1/2}$ = 55 a) which has a similar fission yield [4,5].

In supernova explosions ^{126}Sn is predominantly produced by rapid neutron capture (*r* process). Searches for presence of live ^{126}Sn at the time of condensation of solar matter by the detection of excess or depletion of its stable daughter nuclide ^{126}Te in meteoritic components have so far not met with success (e.g. [6–8]).

A first estimate of $\sim 10^5$ a for the half-life of ^{126}Sn was obtained by [9,10]. The amount of ^{126}Sn produced by neutron irradiation of ^{235}U was estimated from its extrapolated fission yield and from the number of fission events calibrated by measurement of ^{90}Sr. The activity of ^{126}Sn was determined from the activity of ^{126m}Sb + ^{126}Sb at secular equilibrium with its parent nuclide. A more detailed measurement using a similar method has been published recently by [11], which resulted in a half-life of $(2.5 \pm 0.2) \times 10^5$ a (analytical uncertainties are quoted at the 1σ level unless stated differently).

The experiment described in the present study has been performed on an aliquot of the material used for the previous half-life measurement described by [1,12]. The sample was originally separated from spent fuel rods of a nuclear power reactor. An activity concentration of (4.97 ± 0.15) Bq ^{126}Sn/mg Sn has been determined for this material by measuring the activity of ^{126m}Sb + ^{126}Sb in secular equilibrium with ^{126}Sn [1]. The dominant contributions to the overall uncertainty of the activity measurement originate from corrections in coincidence summing (for details, see [1]). The isotopic abundance of ^{126}Sn was determined by accelerator mass spectrometry (AMS), which resulted in ^{126}Sn/Sn = $(9.23 \pm 0.87) \times 10^{-6}$ [12]. The relatively large uncertainty of the abundance measurement is mainly due to the uncertainty in the correction for mass dependent bias and dominates the overall error of the half-life obtained from these data $(2.07 \pm 0.21) \times 10^5$ a [1,12].

The existence of analytical methods for the precise measurement of Sn isotopic composition by thermal ionization mass spectrometry (TIMS) [13,14] led us to attempt a redetermination of the ^{126}Sn abundance in the sample material used for the previous experiments [1,12]. The aim was to reduce the error of the isotopic abundance measurement to a level where it would become an insignificant contribution to the overall uncertainty of the decay constant.

2. Experimental procedures

2.1. Instrumentation

The isotopic abundance measurements were performed on a Finnigan MAT 262 magnetic sector mass spectrometer equipped with an adjustable multicollector system consisting of nine Faraday cups (FCs) and two discrete-dynode secondary electron multiplier (SEM) detectors (model AF150HM9, ETP Electron Multipliers Pty. Ltd., Sydney, Australia). The central ion beam can be deflected into a FC or a SEM detector positioned at either side of the beam axis by means of an electrostatic condenser, whereas the undeflected central beam passes through a retarding potential quadrupole (RPQ) lens system onto the second SEM detector. The RPQ system acts as an energy filter and eliminates ions with irregular flight paths, reducing baseline contributions by peak tails and scattered ions to $< 1 \times 10^{-8}$ at mass (238 ± 1) u at nearly 100% ion transmission. The peak-top flatness is adjustable to better $\pm 0.05\%$ over a range equivalent to $\Delta M/M = \pm 1.5 \times 10^{-4}$ from the peak center. The SEM output signals can be recorded either in analog or in ion-counting mode. Isotopic ratios were obtained by a combination of FC and RPQ measurements, the latter being performed in ion-counting mode. The SEM gain was set to about 2×10^7 electrons per ion in order to ensure that $\sim 99\%$ of the incident ions generated pulses passing the discriminator level at -2.7 mV.

2.2. Sample preparation, filament loading techniques, and isobaric interference problems

The low ^{126}Sn abundance of 9×10^{-6} determined by AMS required us to pay special attention to ion yield and spectral integrity of the mass spectrometric measurements. Potential interference at mass position 126 was expected from $^{126}(CaPO_3)^+$ and $^{126}Te^+$, the latter having been detected in the previous AMS experiments [12]. Furthermore, contributions from hydrocarbons were also anticipated. The use of a liquid N_2 cold trap in the source compartment of the mass spectrometer considerably reduces the hydrocarbon background, but does not totally eliminate the problem.

For elements characterized by relatively high ionization potentials such as tin (7.3 eV), silica gel–H_3PO_4 based activators in combination with rhenium single-filament configuration are commonly used to enhance ionization yields for TIMS applications. For high-precision determination of Sn isotope abundance, however, [13,14] have replaced H_3PO_4 by H_3BO_3 in order to avoid a major isobaric interference at mass 119 caused by the $^{40}Ca^{31}P^{16}O_3^+$ ion (abundance: 93.3%). As $CaPO_3^+$ also interferes at mass 126 (0.000 015 6%) and at mass 128 (0.000 212%), which is used for monitoring Te, this method was adopted for preliminary testing. Because of substantial hydrocarbon contributions to mass 126 throughout the temperature interval of optimal signal intensity (~1300–1400 °C), the H_3BO_3 method had to be abandoned and the standard silica gel–H_3PO_4 loading technique was used for all experiments.

The fission sample was obtained in the form of metal beads [1]. From this material 0.6 mg were dissolved in 5 M HCl (1.9 μg Sn/10 μl solution). Aliquots equivalent to 2 μg Sn were evaporated to near dryness after addition of 2 μl of 0.25 M H_3PO_4. The residues were mixed with 2 μl of a silica gel–H_3PO_4 solution prepared from high-purity H_2O, H_3PO_4, (Merck suprapure) and $SiCl_4$ (99.999% pure, Alfa Research Chemicals) in volumetric proportions of 1000:17:20 [15]. The mixtures were loaded onto outgassed zone-refined Re single filaments, dried and heated in air for 1 s at faint reddish glow. Under automatic control by the mass spectrometer software, filament temperatures were linearly raised to 1320 °C over a period of 30 min and the resulting Sn ion currents (typically in the lower 10^{-13} A range) used to optimize the peak-top flatness of the RPQ system. Over a time period of 1–2 h, temperatures were manually increased to 1400–1430 °C until hydrocarbon contributions to the mass range of interest were essentially eliminated or sufficiently reduced to permit digital data acquisition to be started (see next paragraph). Because the Sn beams were slowly decaying at this stage, filament temperatures were repeatedly increased to maintain sufficient intensity. Over the resulting temperature range of 1400–1550 °C, Sn ion currents averaged 0.37×10^{-11} A [observed range: $(0.08-0.89) \times 10^{-11}$ A], for average data collection periods of 4 h (range: 3–6 h per sample load). The corresponding average count rate at ^{126}Sn was 245 cps (range: 53–580 cps).

In order to evaluate the integrity of the spectral background across masses 112–128, tests were carried out with 2 μg loads of Sn prepared from high purity metal foil and with activator only (filament blank run). Surprisingly, contributions from $CaPO_3^+$ were essentially absent from both the filament blank run and the runs of Sn metal foil throughout the temperature interval of interest (1400–1550 °C), owing to the high purity of the materials used. Similarly, no Sn related signals could be detected in the blank filament run. This is certainly a consequence of low ionization efficiency, but also proves that loading blank contributions are insignificant ($<$1 ppm relative to sample amounts). On the other hand, signals from $CaPO_3^+$ were always present in fission-sample runs, so that masses 126 and 128 had to be corrected using mass 127 (abundance: 0.1857%) as a monitor peak for this compound ion.

Whereas hydrocarbon masses were abundant at temperatures $<$1300 °C, they became rather negligible at temperatures $\geq$1400 °C. Under these conditions, contributions to the high mass side of natural Sn peaks and at mass positions 121 and 123 were $<$10 cps. Masses 126–128 were typically devoid of hydrocarbon background at 1300–1400 °C. Subsequent to increases in filament temperature, however, hydrocar-

bon signals up to several 10 cps did appear, which peaked at mass positions located ~0.2 u above the peaks of interest [^{126}Sn, ^{127}($CaPO_3$), and ^{128}Te], but were decaying to less than 1 cps within a few minutes. At the given mass offset and the working resolution of the mass spectrometer (~570, 10% valley convention), these hydrocarbon signals are relatively well resolved from the masses of interest. Nevertheless we only have accepted data when the hydrocarbon signals at ^{126}Sn + 0.2 u were <1 cps.

Transient signals of up to 40 cps were observed at 1400–1450 °C at the precise mass position of ^{128}Te in one of the runs of standard (metal foil) Sn and in one sample run (run 1, Table 3). These signals were not related to ^{128}($CaPO_3$) and disappeared completely within a time interval of ~40 min. Because there was no correlated variation of mass 126 intensity, we conclude that the unidentified mass was not ^{128}Te (abundance: 31.8% versus 18.8% for ^{126}Te [16]). This observation renders any ^{128}Te based interference correction for mass 126 problematical. For the sample runs, however, the ^{128}($CaPO_3$) corrected residual signals at mass 128 were sufficiently small, so that, with the exception of the initial part of run 1, interference corrections based on natural Te isotopic composition have a negligible effect on the final results (see Sec. 3).

2.3. Mass-spectrometric data acquisition

A mixed multicollector-static and magnet-switching mode was adopted for the isotopic measurements. After the simultaneous measurement of masses 117, 118, 119, 120, 122, and 124 on the FCs for 4 or 8 s, the magnetic field was switched to sequentially measure mass 124 (if its intensity was $<1.6 \times 10^{-13}$ A), 126, 127, and 128, using the RPQ system in ion counting mode. Integration time was 2 or 4 s for mass 124, 16 s for mass 126, and 4 s for masses 127 and 128. Ten repetitive scan sequences form a data set, yielding ten individual ratio values for simultaneously measured masses and nine values by quadratic interpolation of sequentially measured masses. Run mean values and associated uncertainties are derived from multiple sets as described in Sec. 3. The FC readings were baseline corrected by monitoring the electronic background for 64 s before and after each set with the ion beam shut off by closing the valve between the source and the analyzer section of the instrument. The typical noise levels of the FCs are equivalent to 4×10^{-16} A (1 standard deviation) for 1 s integration. The dark-count rate for the SEM detector was initially very low (0.25 cpm when run 1 was performed). Over a period of 8 months, the dark-count rate increased to 5 cpm and required correction of the SEM data (runs 2 and 3). The atomic ratios involving SEM readings were corrected for intensity-dependent gain bias (see Sec. 2.4.). The observed ratios of $124_{FC}/124_{SEM}$ were used for internal gain correction of the SEM readings. If beam intensities at ^{124}Sn exceeded 1.6×10^{-13} A (= 10^6 cps), mass ^{112}Sn (abundance: 1.0%) was measured instead of ^{124}Sn (5.8%) for 2 or 4 s on the SEM and for 4 or 8 s on a FC, respectively, using $112_{FC}/112_{SEM}$ for SEM gain correction. Gain calibration values for the FC amplifiers established by a factory-built calibration system were typically stable to ±10 ppm for 24 h and therefore do not contribute to the analytical uncertainty. An exponential mass fractionation model [17] and ^{124}Sn/^{118}Sn = 0.239 036 [16] were adopted for correction of thermal mass-dependent fractionation. Mass positions 127 and 128 served for monitoring and correction of isobaric interference at ^{126}Sn by $CaPO_3^+$ and by Te^+ (see Sec. 2.2). From 10 to 20 data sets (=100–200 scans total) each, run mean values and associated uncertainties were calculated from the weighted means of the sets (Table 3).

2.4. SEM related bias corrections

The observed SEM readings were first corrected for dead-time related count losses using the function $i = j/(1 - j\tau)$ appropriate for nonextendable (nonparalyzable) dead-time circuitry [18], where i and j are the incident ion and registered pulse rates, respectively, and τ is the manufacturer-supplied dead-time value (33.9 ns). Results obtained on isotope standards, in particular on the well calibrated National Bureau of Standards (NBS) SRM 982 (equal atom) lead standard [19,20] clearly indicate residual bias after dead-time

correction. Higher ion intensities are enhanced relative to signals of lower intensity, whereas there is no resolvable mass dependent bias in the Pb data as demonstrated by perfect agreement (better than 0.02%) between $^{208}Pb/^{206}Pb$ (=1.000 16) ratios measured on both the SEM and the FC system. Attempts to relate the observed intensity-dependent bias by measurements with a fast digital storage oscilloscope to known sources (ion feedback, ringing, etc.) were not successful. Additional testing of two other multipliers of the same type revealed considerably larger bias as compared to the detector used for the present project. These measurements suggested that the magnitude of the offsets was a property of the individual multipliers rather than depending on the discriminator and counting electronics. In the case of paralyzable counting systems, it has been demonstrated that "effective" dead-time values should be determined from actual beam measurements rather than relying upon electronic calibration of the counting circuitry alone [21]. Our isotopic ratio measurements, however, indicated that no unique dead-time value would yield satisfactory corrections over the full dynamic range of ratio sets obtained for the individual multipliers. In view of these observations, a simple empirical algorithm was adopted for correction, where the real ion incidence rate I is approximated by the polynomial $I = a\,i^2 + b\,i$, i being the dead-time and dark-noise corrected count rate and a and b representing (unknown) coefficients. For the ratio $R = I_A/I_B$ of two ion intensities I_A and I_B, $R = r\,(r\,c\,i_B + 1)/(c\,i_B + 1)$, with $r = i_A/i_B$ and $c = a/b$.

The single correction coefficient c is readily determined from measurements of standard materials with ratios $\neq 1$. The NBS SRM 982 Pb isotopic standard is ideal for this purpose, because $^{207}Pb/^{206}Pb = 0.467\,07$ and $^{204}Pb/^{206}Pb = 0.027\,219$ [19] provide for a convenient dynamical range of observation, and $^{208}Pb/^{206}Pb = 1.000\,16$ can be used for the correction of thermal mass fractionation effects. Table 1 shows the results of three such calibrations carried out over a period of 11 months. c is decreasing with time, in parallel with an aging process of the multiplier, which necessitates a consecutive increase of the cascade voltage in order to compensate for gain loss. At a maximum count rate of 1 MHz for ^{124}Sn (SEM gain-calibration link to FC signals) an observed ratio of $^{126}Sn/^{124}Sn = 0.000\,18$ would have required correction by $(+0.24 \pm 0.02)\%$ when measured in October 1996, as compared to $(+0.14 \pm 0.01)\%$ in September 1997. This variation of the correction coefficient has been taken into account by linear interpolation of the calibration results with time. The maximal corrections applied to the determination of ^{126}Sn abundance are comparable to the total uncertainty of the abundance measurement of ^{126}Sn (Table 3).

Table 1
Coefficients for intensity-dependent ratio bias correction of SEM data derived from NBS SRM 982 Pb standard measurements (see text)

Date	^{206}Pb intensity (cps)	c[a]	MSWD[b]
Oct 96	$(1.02–0.95) \times 10^6$	$(-2.36 \pm 0.15) \times 10^{-9}$	1.06
Apr 97	$(1.08–0.61) \times 10^6$	$(-1.79 \pm 0.11) \times 10^{-9}$	1.11
Sep 97	$(1.00–0.42) \times 10^6$	$(-1.39 \pm 0.14) \times 10^{-9}$	1.34

[a] Errors are $1\sigma_{mean}$ external.
[b] MSWD = mean square of weighted deviates.

2.5. Results on NBS SRM 960/NBL CRM 112a uranium standard

In order to assess the accuracy of low abundance measurements by our RPQ-SEM system, three separate loads of the uranium standard (2 μg each) were measured (Table 2). Each scan consisted of a simultaneous measurement of $^{234}U_{SEM}$–$^{235}U_{FC}$–$^{238}U_{FC}$, followed by a SEM measurement of ^{235}U used for internal calibration of FC/SEM gain. The $^{234}U/^{238}U$ ratios were normalized to $^{238}U/^{235}U = 137.88$ using FC data. Our bias-corrected results are in good agreement with values published by four different laboratories over the last few years (Table 2).

3. Results

The results obtained on 3 loads of 2 μg Sn are listed in Table 3 and shown in Fig. 1. Two different

Table 2
NBS SRM 960/NBL CRM 112a uranium standard results

Run	^{234}U intensity [$\times 10^3$ cps]	$^{234}U/^{238}U$ [$\times 10^{-5}$]	MSWD
1	1.1–4.5	5.2855 ± 0.0025[a]	0.61
2	1.6–2.0	5.2858 ± 0.0045[a]	1.04
3	4.3–7.2	5.2843 ± 0.0022[a]	0.81
Mean		5.2849 ± 0.0017[b]	
Edwards et al. (1993) [22]		5.2854 ± 0.0025[c]	
Stirling et al. (1995) [23]		5.288 ± 0.037[d]	
Eisenhauer et al. (1996) [24]		5.290 ± 0.007[e]	
Peate et al. (1996) [25]		5.286 ± 0.016[f]	

[a] External measurement precision, given at the 95% confidence level.
[b] Weighted mean ±95% c.l., internal (includes an error component from the intensity-dependent bias correction; see Sec. 2.4.)
[c] Mean of 8 runs ± $2\sigma_{mean}$, external.
[d] Mean of 6 runs ± $2\sigma_{mean}$, external.
[e] Mean of 11 runs ± $2\sigma_{mean}$, external.
[f] Mean of 5 runs ± $2\sigma_{mean}$, external.

modes have been used to correct the $^{126}Sn/^{118}Sn$ ratios for isobaric contribution. The data on the left-hand side of Table 3 are corrected for $CaPO_3^+$ contributions only, whereas those on the right-hand side include a superimposed correction for tellurium, assuming natural isotopic composition. As has been detailed in Sec. 2.2 the latter correction is problematical, due to the occasional presence of an ion species at mass 128, which has no resolvable correlated contribution to mass 126. Furthermore, because ^{126}Te is shielded by long-lived ^{126}Sn and because the fission yield at mass 126 is lower than that at mass 128, any fission contribution to natural Te would tend to lower $^{126}Te/^{128}Te$. Therefore, an interference-correction based on natural isotopic abundance of Te is likely to overcorrect the data. Fortunately, the residual signals at mass 128 after correction for $CaPO_3^+$ were so small [128/118 varying from (0–0.21) $\times 10^{-6}$] that even a natural Te based interference correction has a negligible effect on the

Table 3
Atomic ratios normalized by $^{124}Sn/^{118}Sn = 0.239\ 036$ [16]

Run	^{126}Sn (cps)	$^{126}Sn/^{118}Sn$			
		Corrected for $CaPO_3$	MSWD	Corrected for $CaPO_3$ and Te	MSWD
1	55–350	$(4.317 \pm 0.006) \times 10^{-5}$	3.1	$(4.318 \pm 0.006) \times 10^{-5}$[a]	3.6
2	60–350	$(4.316 \pm 0.008) \times 10^{-5}$	2.7	$(4.313 \pm 0.009) \times 10^{-5}$	2.9
3	95–560	$(4.321 \pm 0.005) \times 10^{-5}$	1.2	$(4.315 \pm 0.005) \times 10^{-5}$	1.3
Pooled mean		$(4.318 \pm 0.004) \times 10^{-5}$[b]	2.5	$(4.317 \pm 0.004) \times 10^{-5}$[c]	2.7

Mean values are calculated by use of weighting function $(s_i^2 + V_{ext})^{-1}$, where s_i denotes the standard external error of data set i and V_{ext} is a constant external variance term (see text). All errors given as $1\sigma_{mean}$.

Pooled Faraday measurements: $^{117}Sn/^{118}Sn = 0.316\ 79 \pm 0.000\ 01$ MSWD = 2.3 (0.31682 [13]; 0.31673 [16])
$^{119}Sn/^{118}Sn = 0.354\ 22 \pm 0.000\ 12$[d] MSWD = 1.7 (0.35460 [13]; 0.35458 [16])
$^{120}Sn/^{118}Sn = 1.345\ 99 \pm 0.000\ 03$ MSWD = 1.5 (1.34599 [13]; 1.34601 [16])
$^{122}Sn/^{118}Sn = 0.191\ 25 \pm 0.000\ 01$ MSWD = 1.0 (0.19128 [13]; 0.19125 [16])

The ratios in parentheses are given for reference and are calculated from Rosman et al. (1984) [13] and Lee and Halliday (1996) [16].
[a] The first four data sets have been omitted from this run because of a transient isobaric interference at mass 128 observed in sets 1 and 2 (see text).
[b] 95% confidence limits external: $\pm 0.007 \times 10^{-5}$.
[c] 95% confidence limits external: $\pm 0.008 \times 10^{-5}$.
[d] Large correction for $^{119}(CaPO_3)^+$ (see text).

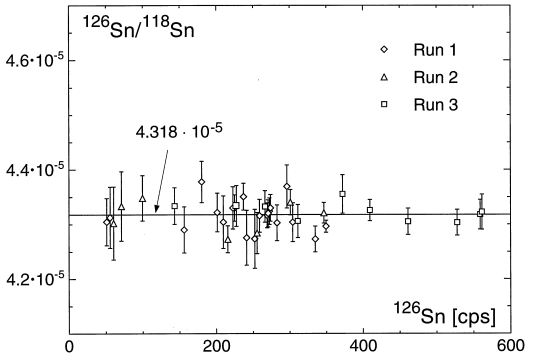

Fig. 1. Plot of the set mean values of $^{126}Sn/^{118}Sn$ from the three sample measurements (corrected for $CaPO_3^+$ only, see text) vs count rate of ^{126}Sn. Error bars are 2σ. The data show excess scatter but do not correlate with intensity.

data, apart from slightly increasing the scatter (enhanced mean square of weighted deviates [MSWD] values in Table 3).

The mean $^{119}Sn/^{118}Sn$ ratio corrected for contributions from $CaPO_3^+$, 0.354 22 ± 0.000 25, is almost identical with the precise value of 0.354 58 given by [16], in spite of the large interference corrections [the uncorrected $^{119}Sn/^{118}Sn$ ratios vary from 0.37 to 0.66 for $^{127}(CaPO_3)/^{118}Sn = (0.3–6.1) \times 10^{-4}$]. The rather excellent fit indicates that the bulk of the signal monitored at mass 127 is related to $^{127}(CaPO_3)^+$ and that corresponding corrections at mass 126 (which were ≤0.12%) and at mass 128 are appropriate. $^{120}Sn/^{118}Sn$ and $^{122}Sn/^{118}Sn$ are in good agreement with the data of [16], whereas $^{117}Sn/^{118}Sn$ is slightly low compared to the value calculated from [16] and is intermediate between the latter and the ratio calculated from the earlier data of [13].

The mean $^{126}Sn/^{118}Sn$ values of the three runs show excellent reproducibility. The within-run fluctuation of the set mean values, however, tends to exceed statistical expectation, as demonstrated by MSWD values ranging from 1.2 to 3.6. Fig. 1 shows the pooled individual set mean ratios plotted versus ^{126}Sn count rate. The ratios do not correlate with count rate. On the other hand, excess scatter is clearly visible, but is rather randomly distributed. We therefore have chosen to evenly distribute an external variance component V_{ext} among the data sets i which is not correlated with precision. This is accomplished by the weighting function $(s_i^2 + V_{ext})^{-1}$ which must satisfy the condition MSWD = 1 [26]. In view of the "randomness" of the data distribution, we believe that this special weighting procedure leads to a reasonable approximation of the precision of the mean values. We thus adopt $^{126}Sn/^{118}Sn = (4.318 \pm 0.004) \times 10^{-5}$ (which includes a SEM gain calibration uncertainty of ±0.02%) as our final result.

4. Discussion

From a ^{118}Sn abundance value of 24.2178% [16], we obtain $^{126}Sn/Sn = (10.457 \pm 0.009) \times 10^{-6}$. At the 2σ error level, the result agrees with the value of $(9.23 \pm 0.87) \times 10^{-6}$ established by the previous AMS measurement [12]. The latter has a significantly larger systematic uncertainty originating from a combination of non-linear mass dependent processes such as the formation of negative ions in the source, the stripping process in the high voltage terminal and the ion transport from the source to the detector. These complications have limited the accuracy of the previous isotopic ratio determination by AMS to ~10%. For elements, which are efficiently ionized by thermal ionization, TIMS or ICP-MS techniques may therefore be preferable for the measurement of ratios $<10^6$.

Using the activity concentration value of (4.97 ± 0.15) Bq $^{126}Sn/mg$ Sn given by [1] and the atomic weight of 118.71 g Sn/mol, $\lambda(^{126}Sn)$ is $(9.37 \pm 0.28) \times 10^{-14}$ s^{-1}. Compared to the uncertainty of the activity concentration, the contribution from the new abundance determination is negligible. With a conversion factor of 3.1557×10^7 s/year, we obtain

$$T_{1/2} = (2.345 \pm 0.071) \times 10^5 a (1\sigma).$$

The new precise half-life for ^{126}Sn is in good agreement with the recent result of $(2.5 \pm 0.2) \times 10^5$ a obtained by Zhang et al. (1996) [11] which is based on fission yield estimates rather than on a direct measurement of the isotopic abundance of ^{126}Sn.

Acknowledgements

The authors thank H. Baur for numerous discussions related to ion-counting problems as well as two anonymous reviewers for their constructive comments. This work was supported in part by the Swiss National Science Foundation.

References

[1] P. Haas, P. Gartenmann, R. Golser, W. Kutschera, M. Suter, H.-A. Synal, M.J.M. Wagner, E. Wild, G. Winkler, Nucl. Instrum. Methods B 114 (1996) 131.
[2] S.R. Taylor, S.M. McLennan, The Continental Crust: Its Composition and Evolution, Blackwell, Oxford, 1985, p. 46.
[3] T.W. Melnyk, J. McMurry, F.P. Sargent, High Level Radioactive Waste Management: Proceedings of the Fifth Annual International Conference 3, LaGrange Park, IL, 1994, p. 1222.
[4] M. Koide, E.D. Goldberg, J. Environ. Radioactiv. 2 (1985) 261.
[5] T.L. Patton, W.R. Penrose, J. Environ. Radioactiv. 10 (1989) 201.
[6] D. Heymann, M. Dziczkaniec, Geochim. Cosmochim. Acta 45 (1981) 1829.
[7] C.L. Smith, J.R. De Laeter, Meteoritics 21 (1986) 133.
[8] R.D. Loss, K.J.R. Rosman, J.R. De Laeter, Geochim. Cosmochim. Acta 54 (1990) 3525.
[9] C.J. Orth, B.J. Dropesky, Bull. Am. Phys. Soc. 3 (1958) 207.
[10] B.J. Dropesky, C.J. Orth, J. Inorg. Nucl. Chem. 24 (1962) 1301.
[11] S. Zhang, J. Guo, A. Cui, D. Li, D. Liu, J. Radioanal. Nucl. Chem. 212 (1996) 93.
[12] P. Gartenmann, R. Golser, P. Haas, W. Kutschera, M. Suter, H.-A. Synal, M.J.M. Wagner, E. Wild, Nucl. Instrum. Methods B 114 (1996) 125.
[13] K.J.R. Rosman, R.D. Loss, J.R. De Laeter, Int. J. Mass Spect. Ion Processes, 56 (1984) 281.
[14] K.J.R. Rosman and N.J. McNaughton, Int. J. Mass Spectrom. Ion Processes 75 (1987) 91.
[15] R.D. Tucker, unpublished.
[16] D.-C. Lee, A.N. Halliday, Int. J. Mass Spectrom. Ion Processes 146 (1995) 35.
[17] W.A. Russell, D.A. Papanastassiou, T.A. Tombrello, Geochim. Cosmochim. Acta 42 (1978) 1075.
[18] J.W. Müller, Nucl. Instrum. Methods 112 (1973) 47.
[19] E.J. Catanzaro, T.J. Murphy, W.R. Shields, E.L. Garner, J. Res. Natl. Bur. Stand. Sect. A 72 (1968) 261.
[20] W. Todt, R.A. Cliff, A. Hanser, A.W. Hofmann, in Earth Processes: Reading the Isotopic Code, Geophysical Monograph, 95 (1996) 429.
[21] J.M. Hayes, D.E. Matthews, D.A. Schoeller, Anal. Chem. 50 (1977) 25.
[22] R.L. Edwards, J.W. Beck, G.S. Burr, D.J. Donahue, J.M.A. Chappell, A.L. Bloom, E.R.M. Druffel, F.W. Taylor, Science 260 (1993) 962.
[23] C.H. Stirling, T.M. Esat, M.T. McCulloch, K. Lambeck, Earth Planet. Sci. Lett. 135 (1995) 115.
[24] A. Eisenhauer, Z.R. Zhu, L.B. Collins, K.H. Wyrwoll, R. Eichstätter, Geol. Rundsch. 85 (1996) 606.
[25] D.W. Peate, J.H. Chen, G.J. Wasserburg, D.A. Papanastassiou, J.W. Geissman, Geophys. Res. Lett. 23 (1996) 2271.
[26] K.R. Ludwig, USGS Open-File Report No. 91-445 (1994) p. 30.